Epigenetics & Chromatin

RESEARCH

Open Access

LSD1 induces H3 K9 demethylation to promote adipogenesis in thyroid-associated ophthalmopathy

Yuyan Xu[3†], Jing Hu[1,2†], Yuhang Fan[4†], Licheng Sun[1,2], Ning Shen[1,2], Qihuang Jin[1,2], Ling Zhang[4*], Jin Zhang[3*], Fang Zhang[1,2*] and Hui Chen[1,2*]

Abstract

Background Thyroid-associated ophthalmopathy (TAO) is an autoimmune orbital disease influenced by multiple factors, including genetic and immune factors. The enlargement of orbital fat tissues are mainly due to abnormal activation of adipocyte differentiation. Epigenetic modifications provide mechanistic insight for regulating gene expression and cellular differentiation. Lysine specific demethylase 1 (LSD1) is reported in regulation of adipogenesis. Therefore, it is critical to investigate the relationship between epigenetic modifier LSD1 and histone modification level during TAO process.

Results In this study, combined with the clinic study and highthrough sequencing approach, our results revealed that the volume of orbital fat tissue was lower in TAO patients compared to non-TAO patients, whereas the number of adipocytes was higher in TAO patients compared to non-TAO patients, the expression level of adipocyte differentiation markers were higher in TAO samples. Consistently, at the cellular system, the expression level of adipogenic markers were higher in the TAO derived cells compared with the non-TAO cells. And we found LSD1 was highly expressed in TAO-derived cells. However, knocking down LSD1 decreased the expression of adipocyte markers. Mechanistically, LSD1 promoted adipocyte gene activation by demethylating H3K9me2 at the promoter regions. Finally, treatment with pargyline, an LSD1 inhibitor, inhibited adipogenesis in a dose-dependent manner, and the same inhibition of adipogenesis results were obtained with treatment with *t*eprotumumab alone or combined with pargyline.

Conclusions Overall, our study indicates that epigenetic modifications were dysregulated in TAO process, and these data elucidated a novel mechanism of adipocyte differentiation during TAO progression and positioned LSD1 as a potential anti-adipogenesis target in TAO. Further understanding of the interaction betwen transcription factors and epigeneic modifiers or other histone modifications in TAO is essential for providing new perspectives in TAO mechanistic study and clinical intervention.

Keywords Thyroid-associated ophthalmopathy, Adipogenesis, LSD1, H3 K9 me2

†Yuyan Xu, Jing Hu and Yuhang Fan are co-first authors of this manuscript.

*Correspondence:
Ling Zhang
zlingsea@163.com
Jin Zhang
zhgene@zju.edu.cn
Fang Zhang
zhangfang2018@sjtu.edu.cn
Hui Chen
352477354@qq.com
Full list of author information is available at the end of the article

© The Author(s) 2025. **Open Access** This article is licensed under a Creative Commons Attribution-NonCommercial-NoDerivatives 4.0 International License, which permits any non-commercial use, sharing, distribution and reproduction in any medium or format, as long as you give appropriate credit to the original author(s) and the source, provide a link to the Creative Commons licence, and indicate if you modified the licensed material. You do not have permission under this licence to share adapted material derived from this article or parts of it. The images or other third party material in this article are included in the article's Creative Commons licence, unless indicated otherwise in a credit line to the material. If material is not included in the article's Creative Commons licence and your intended use is not permitted by statutory regulation or exceeds the permitted use, you will need to obtain permission directly from the copyright holder. To view a copy of this licence, visit http://creativecommons.org/licenses/by-nc-nd/4.0/.

Graphical Abstract

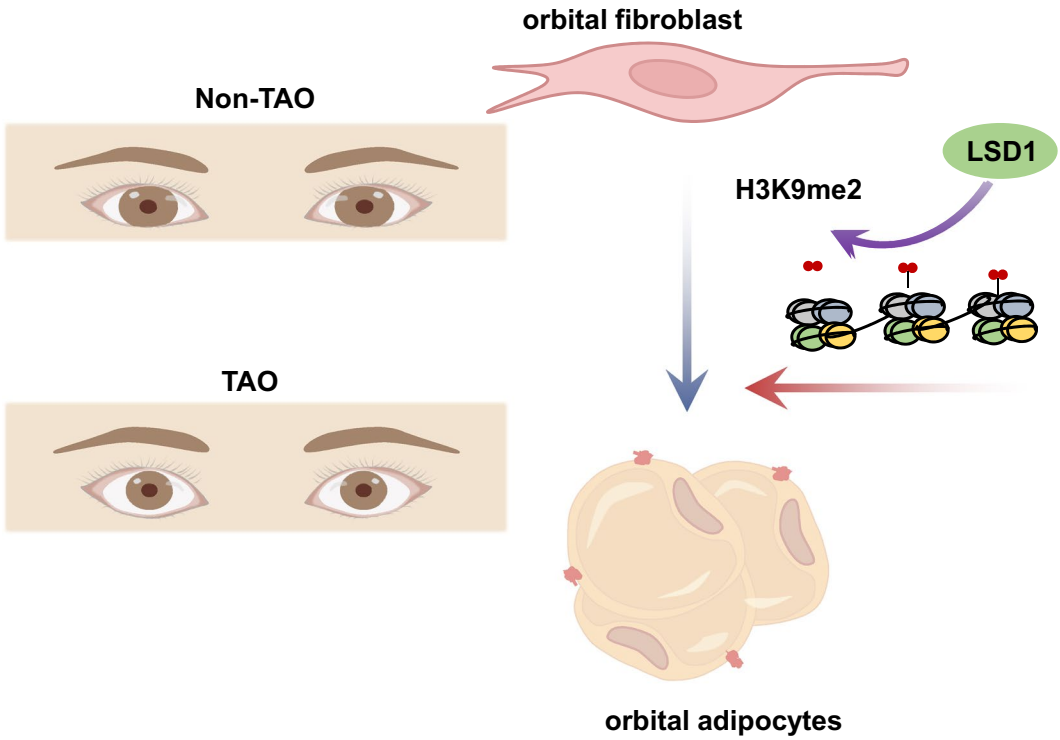

Introduction

TAO, also referred to as Graves'orbitopathy, is a prevalent autoimmune disorder [1–3] frequently manifested as eyelid retraction, exophthalmos, and double vision. In severe cases, it can elicit corneal ulceration and decrease visual acuity [1, 4]. Mechanistically, these syndromes result from the enlargement of extraocular muscles and orbital adipose tissues [1]. Notably, earlier studies have established that orbital fibroblasts are major targets in TAO pathogenesis [5]. They are heterogeneous and display different surface markers, such as CD34, CD40, thyrotropin receptor, and insulin-like growth factor-1 (IGFR-1) receptor [6]. The release of cytokines and chemokines drives the activation of surface markers, resulting in the synthesis of glycosaminoglycans, such as hyaluronan, which, in turn, induce tissue swelling and TAO [7].

The differentiation of preadipocytes to mature adipocytes is governed by transcription factors such as CCAAT/enhancer binding proteins (C/EBPs) and peroxisome proliferator-activated receptor gamma (PPARγ) under adipogenic stimuli. The coordination of these transcription factors maintains adipocyte gene expression, including fatty acid binding protein 4 (*FABP4*) and adiponectin (*ADIPOQ*) [8, 9]. Previous studies have determined that cells isolated from orbital fat tissues in TAO are susceptible to adipogenesis upon stimulation [10, 11]. However, orbital adipose fibroblasts are heterogeneous in terms of surface receptor expression [12]. Their morphology and gene transcript profiles are distinct from those in different regions of the human body in response to inflammatory factors, hormones, and prostaglandins [12, 13], indicating that the molecular mechanism underlying adipogenesis in TAO is different from those outlined in prior research.

Lysine-specific demethylase 1 (LSD1) was the first demethylase identified and functions as a repressive marker by removing mono- or dimethyl groups from lysine 4 of histone 3 (H3 K4) and as an active marker for demethylating H3 K9 [14–16]. Its activity is modulated by interactions with transcription factors under various physiological processes [14, 17, 18]. Of note, LSD1 mediates embryonic stem cell self-renewal and the

differentiation of adipose tissue [19–21]. According to earlier studies, its high expression indicates a poor prognosis in various cancer types [22, 23]. Nevertheless, the regulatory role of LSD1 in TAO and the molecular mechanism remain elusive.

Therefore, this study aimed to analyze the morphological and molecular features of orbital adipocyte tissues derived from non-TAO and TAO patients. The results also demonstrated that LSD1 was highly expressed in TAO-derived cells and orbital adipocyte tissue collected from TAO patients, whilst knocking down LSD1 expression decreased the expression of adipocyte genes and inflammatory factors. Mechanistically, LSD1 demethylated H3 K9 me2 at the promoter regions of adipocyte differentiation marker genes to activate their expression, leading to adipocyte hypertrophy in TAO. Overall, the current study uncovered a novel mechanism targeting adipogenesis in TAO.

Results

Characteristics of human orbital fat tissues

Adipocyte formation involves the differentiation of mesenchymal stem cells to preadipocyte cells and terminal differentiation. These cells are the primary component of adipocyte tissue [9]. The number and size of adipocytes exhibit significant plasticity under physiological and pathophysiological conditions [24]. Several studies have concluded that orbital fibroblasts derived from TAO patients can serve as preadipocyte cells and undergo adipogenesis. However, the mechanisms that trigger aberrant adipocyte differentiation in TAO remain to be elucidated.

To investigate the effects of the expansion of orbital fat tissues, orbital fat tissues were collected from TAO patients and control participants (non-TAO) undergoing surgical decompression. Histological analysis displayed that the volume of orbital fat tissue was lower in TAO patients compared to non-TAO patients, whereas the number of adipocytes was higher in TAO patients compared to non-TAO patients (Fig. 1A), consistent with the findings of a previous study [11]. As expected, the expression levels of adipocyte differentiation markers, including *PPARγ*, *FABP4*, *PGC1a and CIDEA*, were higher in TAO samples (Fig. 1B). Adipose tissues can be classified into white and brown adipose tissue, each with distinct morphological and functional properties. Noteworthily, a recent study identified another type, namely beige adipose tissue. Molecular analysis revealed that orbital fat tissue expressed high expression levels of several beige fat tissue markers (Fig. 1C). Immune cells located in adipose tissues and adipogenesis promote inflammation [25]. Indeed, the expression levels of inflammatory factors were high in orbital fat tissue (Fig. 1D). Overall, these results indicated that the activity and formation of new adipocytes are increased in TAO.

Role of LSD1-mediated adipogenesis in TAO

To identify regulators underlying adipogenesis in TAO, cells derived from the orbital fat tissue of TAO and non-TAO patients were isolated and immortalized, as outlined in a previous study [11]. At the cellular level, the proliferation rate was comparable between the non-TAO and TAO groups (Extended Fig. 1 A). On the other hand, the expression levels of inflammatory factors and adipogenic markers were higher in the TAO group compared to the non-TAO group (Fig. 2A, B), in line with the aforementioned results.

Epigenetic modifications differ across varying cell types, such as precursors and differentiated adipocytes. Thus, epigenetic modulators potentially play a key role in adipogenesis [26]. LSD1 has been reported to regulate the differentiation and activity of adipose tissue [21]. Our results unveiled that LSD1 was highly expressed in TAO-derived cells (Fig. 2C). To further confirm the role of LSD1 in TAO, LSD1 was knocked down in immortalized TAO cells using small hairpin RNA (shRNA) (Extended Fig. 1B). This efficiently reduced the protein levels of LSD1 and substantially decreased the expression levels of inflammatory factors and adipogenesis marker genes (Fig. 2D–F), as well as the quantity of lipid droplets (Extended Fig. 1 C, D). Likewise, the protein level of UCP1 and PGC1α was decreased (Fig. 2G), indicating that LSD1 is a potential regulator of TAO progression.

To elucidate the molecular mechanism by which LSD1 regulates adipogenesis during TAO, the transcriptomic profile of LSD1 was first determined in TAO cells. Therefore, RNA-sequencing was performed in TAO-derived cells, following LSD1 knockdown. The results demonstrated that the expression of 2119 genes was upregulated, whilst that of 3179 genes was downregulated (Fig. 3A, B), including *FABP4, PPARγ, IL6 and IL1B* (Fig. 3C). Gene set enrichment analysis (GSEA) was conducted to assess gene ontology (GO), revealing that genes downregulated following LSD1 knockdown were enriched in biological processes related to lipid metabolism, such as fatty acid biosynthesis and lipid droplet formation (Fig. 3D). Meanwhile, the Kyoto Encyclopedia of Genes and Genomes (KEGG) analysis showed that genes with lower expression levels following LSD1 knockdown were involved in metabolic and immune pathways (Fig. 3E).

Taken together, these results collectively suggested that LSD1 regulated the gene expression of lipid and immune pathways in TAO pathogenesis.

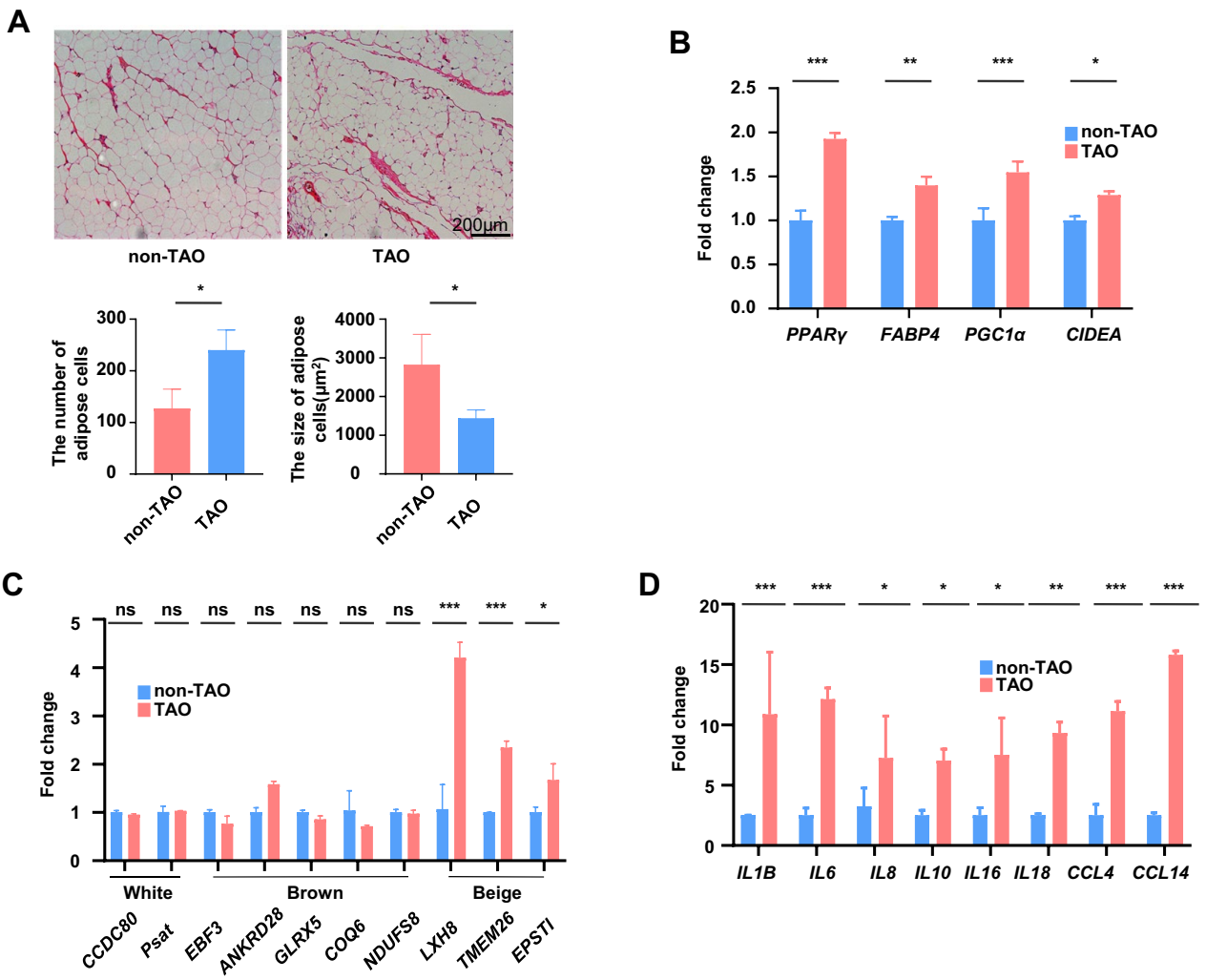

Fig. 1 Characteristics of human orbital fat tissues. The morphology of adipose cells in orbital adipose tissues was observed by H&E staining of non-TAO and TAO patients group, and quantification of the number and size of adipose cells (**A**), scale bar: 200 μm. *p < 0.05, **p < 0.01, ***p < 0.001 according to the unpaired t-test, n = 3 biological repeats. Expression of adipose differentiation genes in normal orbital adipose tissues and in orbital adipose tissues of TAO patients (**B**), *p < 0.05, **p < 0.01, ***p < 0.001 according to the two-way ANOVA test, n = 2 biological repeats. Expression of White, Brown and Beige adipose differentiation genes in normal human orbital adipose tissues and in orbital adipose tissues of TAO patients (**C**), *p < 0.05, **p < 0.01, ***p < 0.001 according to the two-way ANOVA test, n = 2 biological repeats. Expression of inflammatory factors in normal orbital adipose tissues and in orbital adipose tissues of TAO patients (**D**),*p < 0.05, **p < 0.01, ***p < 0.001 according to the two-way ANOVA test, n = 2 biological repeats

LSD1 exerts dual activities, demethylating either H3 K4 me2 or H3 K9 me2, leading to transcription repression or activation, respectively [14, 17]. To investigate the epigenetic status of TAO-derived cells, western blot analysis was initially performed. The results showed that the global level of H3 K9 me2 was lower in TAO-derived cells compared to non-TAO cells (Fig. 4A), whereas LSD1 knockdown in TAO-derived cells increased the levels of H3 K9 me2 (Fig. 4B) and concurrently decreased H3 K4 me2 levels (Fig. 4C), suggesting that LSD1 potentially regulate target gene expression by demethylating H3 K9 me2, activating the expression of inflammatory and adipogenic genes, and promoting TAO progression. To validate this hypothesis, a ChIP-seq assay was performed using an H3 K9 me2 antibody. As anticipated, the enrichment of H3 K9 me2 at the promoter region was lower in TAO-derived cells compared to non-TAO-derived cells (Fig. 4D), while LSD1 inactivation in TAO-derived cells enhanced the enrichment of H3 K9 me2 at the transcriptional start site (TSS) (Fig. 4E), indicative that LSD1 demethylated H3 K9 me2 at the TSS. In addition, GO analysis signaled that genes downregulated

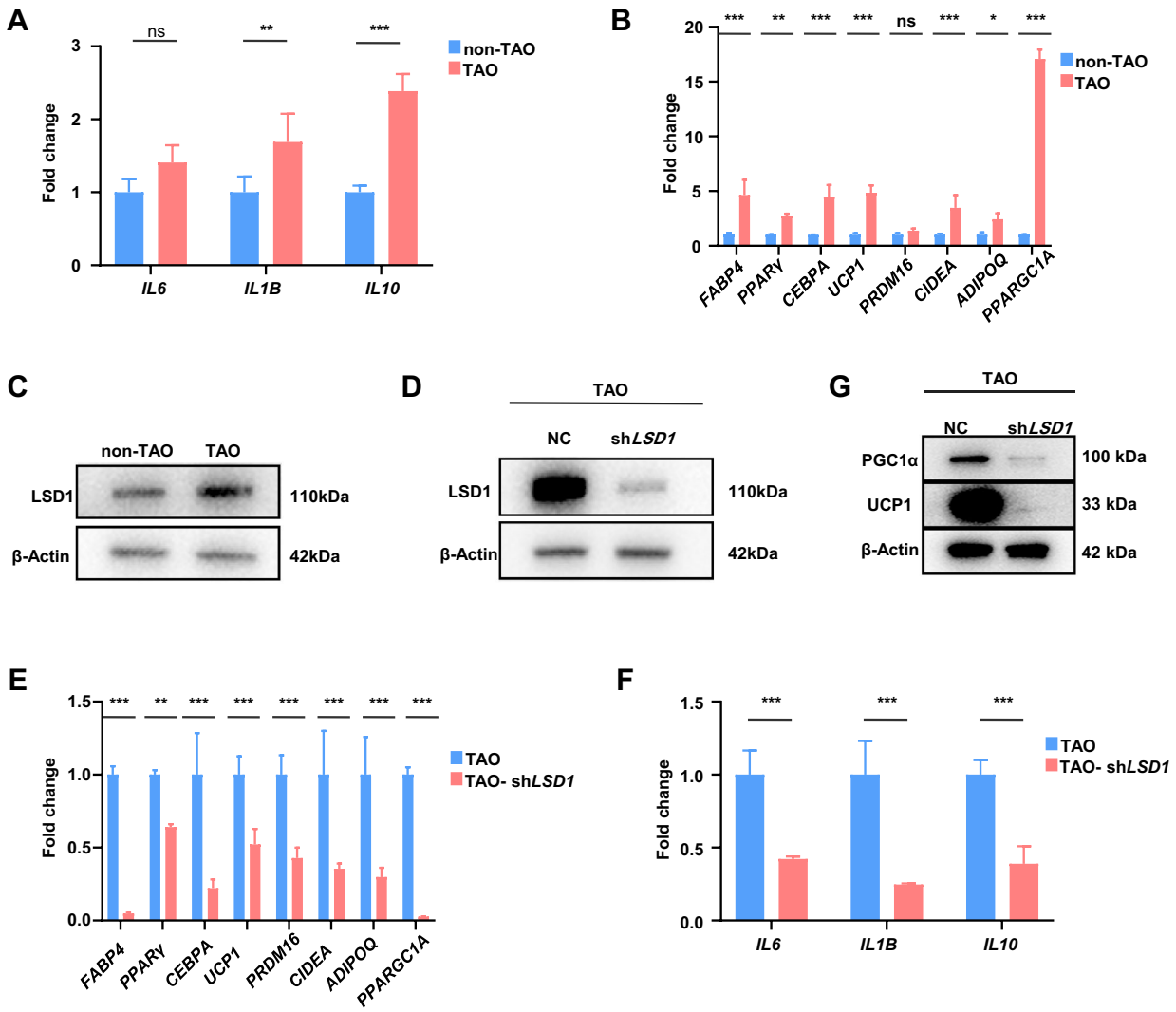

Fig. 2 LSD1 knockdown can inhibit adipocyte differentiation. Expression of Inflammatory factors in normal orbital adipose cells and in orbital adipose cells derived from TAO patients (**A**),*p < 0.05, **p < 0.01, ***p < 0.001 according to the two-way ANOVA test, n = 3 biological repeats. Expression of adipose differentiation genes in normal human orbital adipose cells and in orbital adipose cell derived from TAO patients (**B**), *p < 0.05, **p < 0.01, ***p < 0.001 according to the two-way ANOVA test, n = 3 biological repeats. Western blot analysis of LSD1 protein level in non-TAO orbital adipose cells and TAO orbital adipose cells (**C**). Efficiency detection of lentivirus-mediated LSD1 knockdown in orbital adipose cells derived from TAO patients (**D**). Expression of adipose differentiation genes in TAO orbital adipose cells and TAO orbital adipose cells knocking down LSD1 (**E**), *p < 0.05, **p < 0.01, ***p < 0.001 according to the two-way ANOVA test, n = 3 biological repeats. Expression of inflammatory genes in TAO orbital adipose cells and TAO orbital adipose cells knocking down LSD1 (**F**),*p < 0.05, **p < 0.01, ***p < 0.001 according to the two-way ANOVA test, n = 3 biological repeats. Western blot analysis of UCP1, PGC1α proteins level in TAO orbital adipose cells and TAO orbital adipose cells knocking down LSD1 (**G**)

following LSD1 knockdown were involved in the adipocyte differentiation pathway (Fig. 4F). Specifically, H3 K9 me2 enrichment was lower at the promoter regions of the adipogenic marker gene *FABP4* and inflammatory genes *IL6* and *CCL18* in TAO-derived cells compared to non-TAO-derived cells and was increased following LSD1 knockdown in TAO-derived cells (Fig. 4G, H, Extended Fig. 2 A), implying that LSD1 directly binds and regulates the H3 K9 me2 levels of these genes.

Inactivation of LSD1 enzymatic activity inhibited adipogenesis in TAO

LSD1 can alter the phenotype and metabolic state of adipose tissue and re-encode the fate of adipocytes [27]. The correlation between LSD1 expression and TAO progression positioned LSD1 as a potential target for inhibiting preadipocyte differentiation. To validate this theory, adipogenesis was induced in TAO-derived cells in the presence or absence of the LSD1 inhibitor

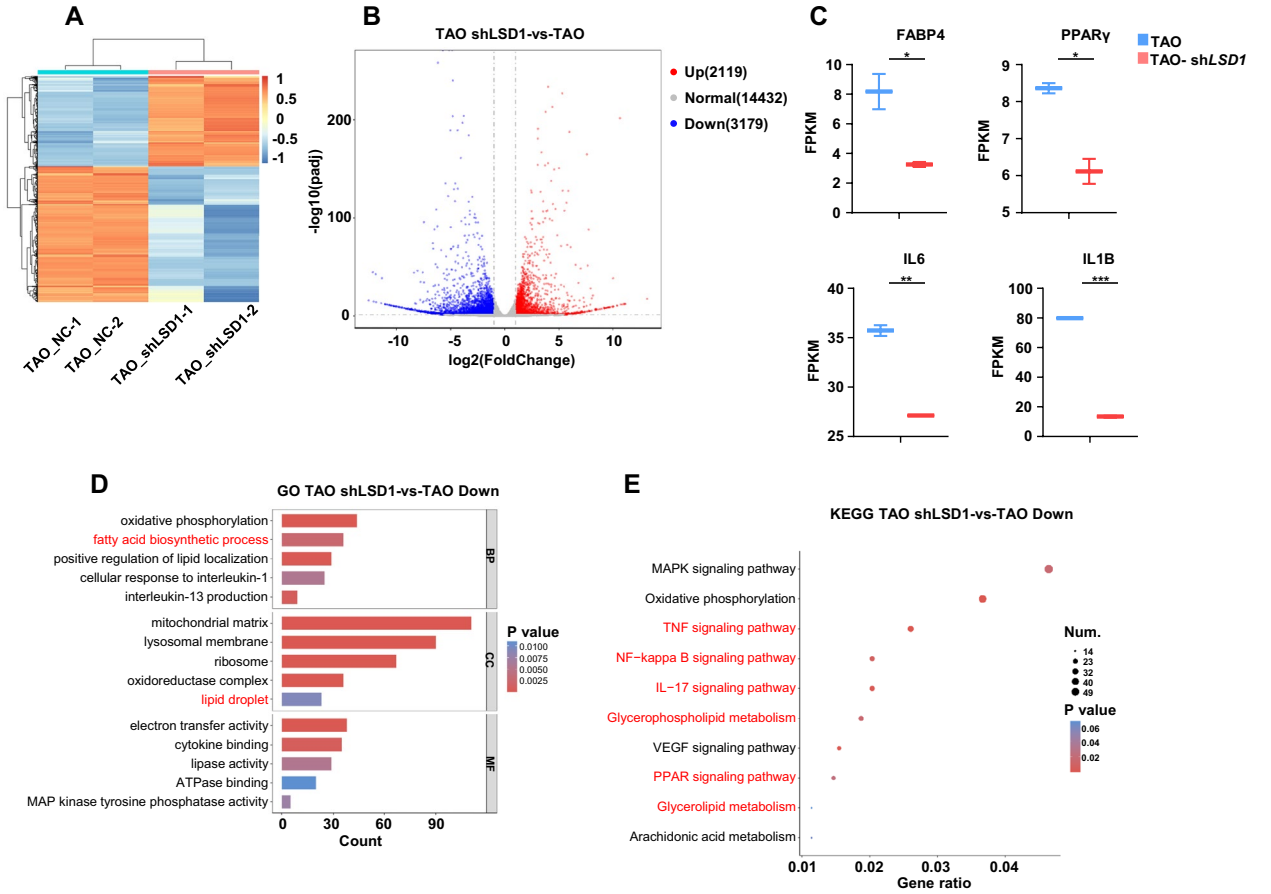

Fig. 3 Transcriptomic analysis of TAO orbital adipose cells after knocking down LSD1. Heatmap of expression level of differentially expressed genes between TAO orbital adipose cells and TAO orbital adipose cells knocking down LSD1 (**A**). Volcano map of differentially expressed genes between TAO orbital adipose cells and TAO orbital adipose cells knocking down LSD1 (**B**), padj < 0.05, |FoldChange|> 2. The presentation of adipocyte differentiation factors and inflammatory factors of TAO orbital adipose cells and TAO orbital adipose cells knocking down LSD1 in the transcriptomic data above (**C**).*p < 0.05, **p < 0.01, ***p < 0.001 according to the unpaired t-test, n = 2 biological repeats. GO analysis of differentially expressed genes between TAO orbital adipose cells and TAO orbital adipose cells knocking down LSD1 (**D**). KEGG analysis of differentially expressed genes between TAO orbital adipose cells and TAO orbital adipose cells knocking down LSD1 (**E**)

pargyline, as well as with dexamethasone, isxobutylmethylxanthine, rosiglitazone, and insulin as outlined in a previous study [11], and the effects of LSD inhibition were monitored by quantifying lipid accumulation using BODIPY staining on day 14. The results showed that the LSD1 inhibitor suppressed lipid droplet formation in a dose-dependent manner at concentrations ranging from 1 μM to 6 μM (Fig. 4I, J). Consistently, the expression levels of adipogenic and inflammatory genes, including *FABP4, UCP1, PRDM16, CIDEA, PPARγ, PPARGC1 A and IL1B*, were decreased (Fig. 5C–I). *T*eprotumumab, a monoclonal antibody used to inhibit insulin-like growth factor 1 receptor (IGF-1R), is FDA-approved for the treatment of TAO [28]. Treatment with *te*protumumab inhibited lipid droplet formation and downregulated the expression of adipogenesis-related genes (Fig. 5A, B, C–H). More importantly, combination treatment with pargyline and teprotumumab exerted an additive inhibitory effect on adipogenesis, as evidenced by the lipid droplet size and the expression of adipogenic markers, whereas no effects were noted on the levels of inflammatory factors(Fig. 5A–I).

These results conjointly showed that LSD1-mediated removal of H3 K9 me2 at the promoter regions of adipogenic markers plays a decisive role in orbital adipogenesis in TAO. Furthermore, the potential anti-adipogenic effects of LSD1 inhibitors showed promise as therapeutic agents for the treatment of TAO.

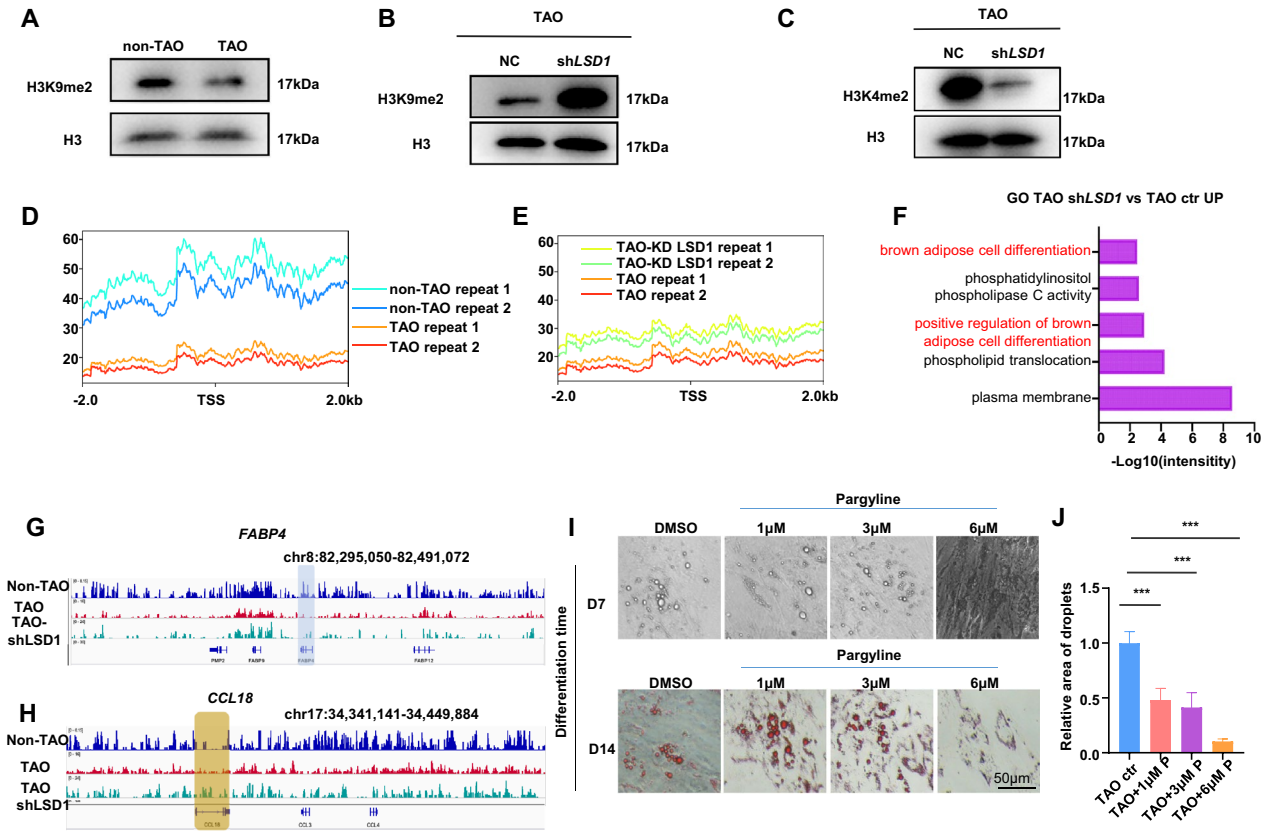

Fig. 4 Role of LSD1-mediated adipogenesis in TAO cells. Western blot analysis of H3 K9 me2 protein level in non-TAO orbital adipose cells and TAO orbital adipose cells (**A**). Western blot analysis of H3 K9 me2 proteins level in TAO orbital adipose cells and TAO orbital adipose cells knocking down LSD1 (**B**). Western blot analysis of H3 K4 me2 proteins level in TAO orbital adipose cells and TAO orbital adipose cells knocking down LSD1 (**C**). The distribution of H3 K9 me2 modification in the promoter region of TAO orbital adipose cells and non-TAO orbital adipose cells (**D**). The distribution of H3 K9 me2 modification in the promoter region of TAO orbital adipose cells and TAO orbital adipose cells knocking down LSD1 (**E**). GO analysis genes with increased histone modification of H3 K9 me2 after LSD1 knockdown in TAO orbital adipocytes (**F**). Modification analysis of H3 K9 me2 on FABP4 gene locus in non-TAO orbital adipose cells, TAO orbital adipose cells and TAO orbital adipose cells knocking down LSD1 (**G**). Modification analysis of H3 K9 me2 on CCL18 gene locus in non-TAO orbital adipose cells, TAO orbital adipose cells and TAO orbital adipose cells knocking down LSD1 (**H**). Representative images of lipid droplet formation when treated with LSD1 inhibitor pargyline (from 1 to 6uM) in TAO cells (**I**) and the quantification of lipid droplets (**J**). scale bar: 50 μm. *p < 0.05, **p < 0.01, ***p < 0.001 according to the one-way ANOVA test, n = 4 biological repeats

Discussion

Herein, LSD1 was highly expressed in orbital adipocyte tissue and immortalized cells derived from TAO patients, while inactivation of LSD1 down-regulated the expression of inflammatory genes and adipocyte marker genes. Mechanistically, LSD1 removed H3 K9 me2 at the promoter regions of genes involved in adipocyte differentiation, leading to the activation of gene expression and promotion of TAO progression. Finally, LSD1 inhibitors repressed adipogenesis in TAO-derived cells.

TAO is an organ-specific autoimmune disease hallmarked by increased adipogenesis, edema, and fibrosis. The results of this study also revealed high expression levels of inflammatory genes. Considering that adipose tissue is an important reservoir for immune cells [25], it is crucial to explore the regulatory relationship between adipocyte markers and inflammatory factors in TAO. Epigenetic modifications (DNA methylation, noncoding RNAs, and histone modification) have been observed to be dysregulated in the receptors of patients with autoimmune-related diseases, including TAO [29]. However, the involvement of epigenetic regulators in TAO remains unknown. LSD1 was first identified to demethylate H3 K4 me2, resulting in transcriptional repression. Besides, it activated gene expression following recruitment by hormone-dependent receptors, including androgen receptor (AR), estrogen receptor (ER) and hormone-independent estrogen-related receptor (ERR) [18]. Given that LSD1 promoted the expression of adipocyte marker genes and inflammatory genes through the removal of H3 K9 me2,

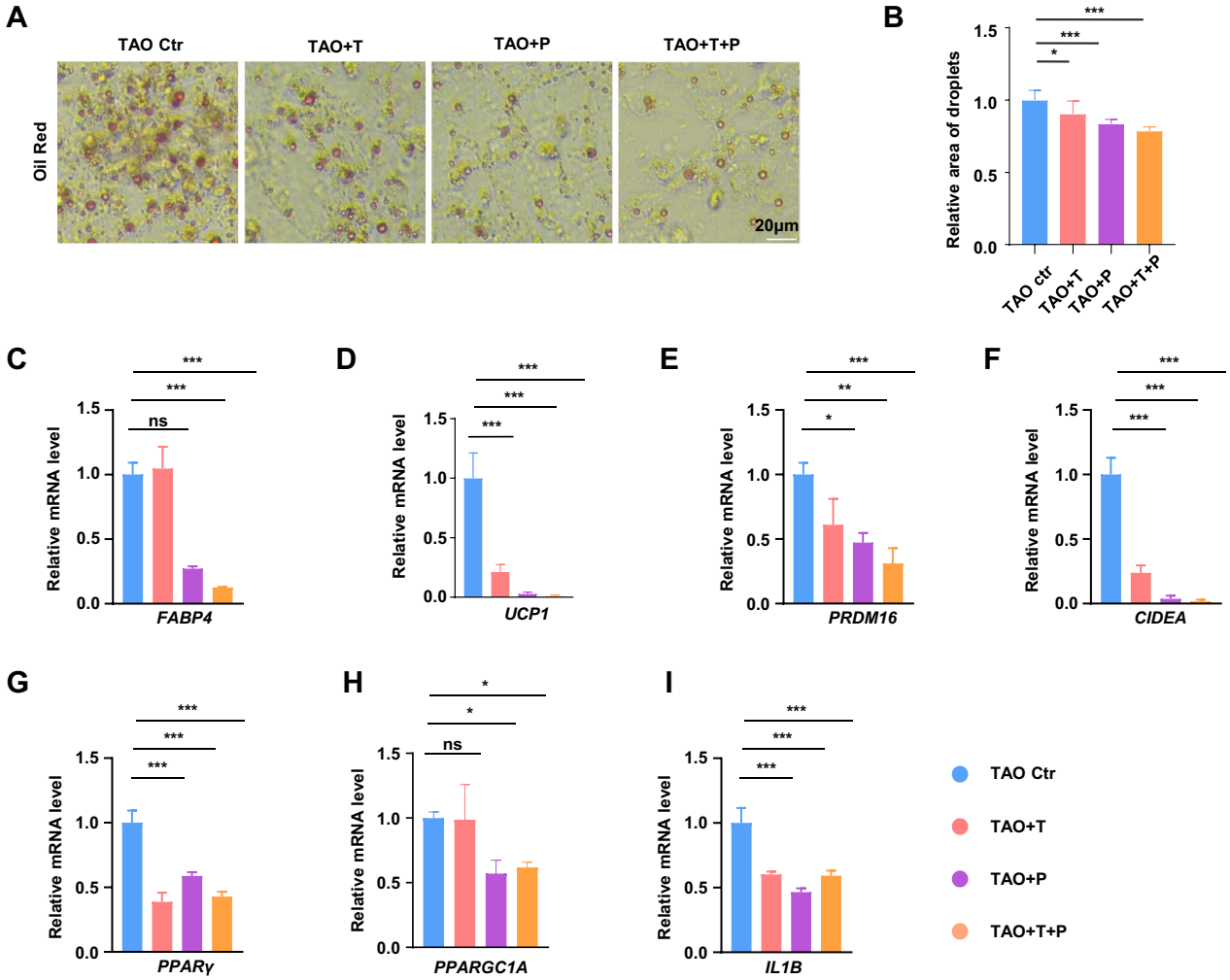

Fig. 5 The combination of LSD1 inhibitor and clinical drugs can effectively reduce the adipogenesis in TAO cells. Representative images of oil red staining of lipid droplets in TAO cells treatment with DMSO, Teprotumumab (T), Pargyline (P), Teprotumumab + Pargyline(T + P) (**A**), scale bar: 20 μm. Quantitative analysis of the number of lipid droplets in A (**B**). *p < 0.05, **p < 0.01, ***p < 0.001 according to the Two-way ANOVA, n = 6 biological repeats. Expression of adipose differentiation genes and Inflammatory factor in TAO cells treatment with DMSO, Teprotumumab (T), Pargyline (P), Teprotumumab + Pargyline(T + P) (**C**–**I**). *p < 0.05, **p < 0.01, ***p < 0.001 according to the two-way ANOVA test, n = 3 biological repeats

the presence of an interaction between LSD1 and TSHR or unknown transcription factors that recruits LSD1 and modulates its enzymatic activity in TAO cannot be excluded. The role of LSD1 in adipocyte differentiation is also associated with energy metabolism [30, 31]. Nevertheless, the impact of LSD1-mediated adipogenesis in TAO formation on cellular metabolism warrants further exploration.

LSD1 has been found to be highly expressed in cancer cells, with epidemiological data suggesting a correlation between high LSD1 expression and poor prognosis [22], thereby implicating the critical role of LSD1 in cancer progression. In the functional analysis, the inactivation of LSD1 enzymatic activity suppressed adipocyte differentiation of TAO-derived cells. Taken together, the current study suggests that LSD1 promotes adipogenesis in TAO progression, with its down-regulation being a potential and promising approach for alleviating aberrant adipogenesis in TAO.

Materials and methods

Ethics statement

This study was approved by the Medical Ethical Committee of Shanghai General Hospital approved this study (research license 2021 KY008) after a thorough evaluation of its scientific merit and ethical justification. All participants voluntarily provided written informed

consent prior to the collection of orbital fat tissue for research purposes. This study adhered to the principles outlined in the Declaration of Helsinki regarding research involving human subjects.

Isolation of human orbital stromal stem cells

Orbital stromal stem cells were isolated from the orbital adipose depot of TAO patients and healthy participants with fat levels within the normal range. Next, the tissue was minced and homogenized using spring scissors. It was then transferred into a 15 mL Falcon tube containing digestion buffer (175 U/mL Collagenase, Type1, Diamond, Cat#A004194), which was subsequently incubated in a 37 ℃ water bath. Afterward, the tube was vortexed every 30 min for 2 h. Then, the tissue slurry was filtered through a 100 μm cell strainer, and digestion was terminated by the addition of 10% fetal bovine serum in DMEM/F12 medium. After centrifuging at 600 rpm for 5 min, the supernatant was discarded, and the stromal vascular fraction (SVF) was resuspended in DMEM/F12 medium supplemented with 10% FBS and 1% penicillin–streptomycin (PS). The medium was changed every three days.

Generation of immortalized human orbital stromal stem cells

Isolated primary preadipocytes were infected with a retrovirus containing TERT plasmid, pBABE-hTERT-Hygro, which expresses hTERT driven by a long-term repeat promoter. 293 T cells were transfected with pBABE-hTERT-Hygro DNA using the PolyJet DNA in vitro transfection reagent. Viral supernatants were collected after 48 h and filtered through a 0.45 μm filter. Afterward, primary adipocytes were infected with supernatant in the presence of 8 μg/mL Polybrene. Lastly, cells were treated with 1000 μg/mL hygromycin B in DMEM/F12 medium containing 10% FBS and antibiotics.

In vitro preadipocyte differentiation

Confluent cells were treated with DMEM/F12 medium supplemented with 10% FBS, 1%PS, 5 μg/mL insulin (#12585014, ThermoFisher Scientific), 1 μM dexamethasone (#D4902, Sigma), 1 μM rosiglitazone (#R2408, Sigma), and 0.5 μM isxobutylmethylxanthine (IBMX) (#13630S, Cell Signaling Technology) for the first 6 days. The medium was replaced with a maintenance medium (DMEM/F12 supplemented with 10% FBS, 1% PS, 1 μM rosiglitazone, and 5 μg/mL insulin) for the subsequent 8 days. The medium was changed every three days until 14 days.

Oil red O staining

After 14 days of differentiation, cells were washed twice with PBS and fixed with 4% paraformaldehyde for 30 min. Lipids were stained using Oil Red O following the manufacturer's protocol (BioVision, Cat#K580), and stained cells were washed five times with PBS and visualized under a microscope (FV3000) for morphological analysis.

RNA isolation and qRCR analysis

Total cells were extracted from cells or tissues using TRIzol (Invitrogen) and reverse-transcribed into cDNA using the Takara PrimeScript RT reagent kit according to the manufacturer's instructions. Quantitative reverse transcriptase PCR (qRT-PCR) was performed using SYBR green fluorescent dye on the ViiA7 Real-Time PCR system (Life Technologies). The 2-ΔΔCt method was used to calculate the gene expression level of each mRNA. Glyceraldehyde-3-phosphate dehydrogenase (GAPDH) served as a reference for normalization. The sequences of primers used in this study are provided as follows:

Gene name	Forwards	Reverse
hPPARg	ACCAAAGTGCAATCAAAGTGGA	ATGAGGGAGTTGGAAGGCTCT
hPPARGC1 A	TGAAGACGGATTGCCCTCATT	GCTGGTGCCAGTAAGAGCTT
hCIDEA	TTATGGGATCACAGACTAAGCGA	TGCTCCTGTCATGGTTGGAGA
hIL1B	TTCGACACATGGGATAACGAGG	TTTTTGCTGTGAGTCCCGGAG
hIL6	ACTCACCTCTTCAGAACGAATTG	CCATCTTTGGAAGGTTCAGGTTG
hIL-1Ra	CATTGAGCCTCATGCTCTGTT	CGCTGTCTGAGCGGATGAA
hIL-8	ACTGAGAGTGATTGAGAGTGGAC	AACCCTCTGCACCCAGTTTTC
hIL-10	GACTTTAAGGGTTACCTGGGTTG	TCACATGCGCCTTGATGTCTG
hIL-18	TCTTCATTGACCAAGGAAATCGG	TCCGGGGTGCATTATCTCTAC
hIL16	GCCGAAGACCCTTGGGTTAG	GCTGGCATTGGGCTGTAGA
hIL18	TCTTCATTGACCAAGGAAATCGG	TCCGGGGTGCATTATCTCTAC
hCCL14	CCAAGCCCGGAATTGTCTTCA	GGGTTGGTACAGACGGAATGG
hCCL4	CTGTGCTGATCCCAGTGAATC	TCAGTTCAGTTCCAGGTCATACA
hFABP4	ACTGGGCCAGGAATTTGACG	CTCGTGGAAGTGACGCCTT
hC/EBPa	AACACGAAGCACGATCAGTCC	CTCATTTTGGCAAGTATCCGA

Gene name	Forwards	Reverse
hADIPOQ	CTGGTGAGAAGGGTG AGAAAG	GTTTCACCGATGTCT CCCTTAG
hCCDC80	GACCCCGTTTCACTA TGCTGT	GGCGAGCTAGTCTCA ACACG
hpSat	GGCCAGTTCAGTGCT GTCC	GCTCCTGTCACCACA TAGTCA
hEBF3	GGGGACGACCATGAA GGAG	CCCCTGCCTATCGTA GAGC
hANKRD28	AATTGCTTGTGTCGC ATGGAG	TAGCAGGCTACATGA AGAGGT
hGLRX5	CTCCGACAAGGCATT AAAGACT	AACTCGCCATTGAGG TACACT
hCOQ6	GTTTTGGTGCCTGGG ACCATA	TCCACGATATAGCCC ATGTCA
hNDUFS8	CCATCAACTACCCGT TCGAGA	CCGCAGTAGATGCAC TTGG
hLXH8	GAATGACCTATGCTG GCATGT	ACCCAGTCAGTAGAA TGGATGTG
hTMEM26	ATGGAGGGACTGGTC TTCCTT	CTTCACCTCGGTCAC TCGC
hEPSTI	ACCCGCAATAGAGTG GTGAAC	GCTATCAAGGTGTAT GCACTTGT

Western blot analysis

Protein extracts were prepared using radioimmunoprecipitation assay (RIPA) buffer supplemented with a protease inhibitor cocktail (1:100, Meilunbio). Tissue samples were homogenized using an ultrasonication machine, and the supernatant was collected. Protein concentration was determined using a BCA protein assay kit (Thermo Fisher Scientific). Approximately 30–60 μg of protein was separated via electrophoresis on 10% and 15% Tris–glycine SDS-PAGE gels and then transferred to a 0.22-μm PVDF membrane (Millipore). The membrane was blocked for 1 h at room temperature using TBST containing 5% skim milk and subsequently incubated overnight at 4 °C with the primary antibody diluted in QuickBlock™ Primary Antibody Dilution Buffer (Beyotime). Afterward, the membrane was incubated with horseradish peroxidase (HRP)-conjugated secondary antibody in 5% skim milk, and the protein bands were visualized using ECL chemiluminescence. Band intensity was quantified using ImageJ software (NIH).

Cell counting kit-8 (CCK-8) assay

Cells (1000/well) were seeded into a 96-well transparent dish. The CCK-8 solution was added to the medium (1:100) and incubated at 37 °C for 4 h. Then, absorbance was determined at 450 nm, and the cell number was derived from the standard curve.

CUT&TAG library generation and sequencing

CUT&TAG was carried out following established protocols using the Hyperactive In-Situ ChIP Library Prep Kit for Illumina (Vazyme Biotech, TD901). Briefly, cells were treated with 10 μL of pre-washed ConA beads in a 1.5-mL low-binding tube. Next, 50 μL of antibody buffer containing 0.5 μg of antibody was added, and the mixture was incubated for 2 h at room temperature. After two washes with dig-wash buffer, 50 μL of dig-wash buffer and 0.5 μg of secondary antibody were added, followed by incubation at room temperature for 30 min. The samples were washed twice with 800 μL of dig-wash buffer, following which 0.58 μL of pG-Tn5 and 100 μL of dig-300 buffer were added. After incubating at room temperature for 1 h, the samples were washed twice with 800 μL of dig-wash buffer. Tagmentation was performed by introducing 300 μL of tagmentation buffer, followed by incubation at 37 °C for 1 h. The reaction was terminated by adding 10 μL of 0.5 M EDTA, 3 μL of 10% SDS, and 2.5 μL of 20 mg/mL Proteinase K. Following phenol–chloroform extraction and ethanol precipitation, PCR was conducted to generate libraries, which were sequenced using Illumina Hi-Seq Xten or Hi-Seq 2500 systems, following the manufacturer's instructions.

RNA sequencing (RNA-seq) analysis

Total RNA was extracted from the cells as previously described. A Nanophotometer NP80 was used to quantify RNA concentration and purity. For RNA sequencing, the RNA samples were analyzed by LC-Biotechnology Co., Ltd. (Hangzhou, China). The final cDNA library had an average insert size of 300 ± 50 bp, and sequencing was conducted using 2× 150-bp paired-end reads (PE150) on an Illumina NovaSeq™ 6000, following the manufacturer's protocol.

The raw RNA-seq data, provided in fastq format, were processed using fastq v0.23.2 with default settings, which involved trimming reads with adapters, excluding low-quality reads, and filtering sequences containing N bases. The cleaned data were then aligned to the GRCh38 (UCSC) genome assembly using STAR v2.7.10a with default parameters. Uniquely mapped read pairs were quantified using featureCounts v2.0.1. The resulting gene count matrix was normalized via quantile normalization using the R package DESeq2 v1.32.0. A log transformation of this matrix was applied for principal component analysis (PCA). Differentially expressed genes (DEGs) were identified using DESeq2, using criteria of adjusted $P < 0.05$ and absolute $\log2|\text{FoldChange}| \geq 1$. KEGG and GO enrichment analyses for the DEGs were conducted using clusterProfiler v4.6.0. Similarly, gene counts, and

P-values for these terms were visualized using clusterProfiler v4.6.0. Significant DEGs were further illustrated through heat maps and bar plots generated using heatmap v1.0.12 and ggplot2 v3.4.0, respectively.

CUT &TAG sequencing analysis

Raw sequencing data was filtered using fastp (version 0.23.1) to discard low-quality reads and trim reads contaminated with adaptor sequences. Clean reads were mapped to the reference genome of Homo from Homo_sapiens.GRCh38.dna.toplevel.fa using bowtie2 (version 2.2.6) with default parameters. Sambamba (version 0.7.1) was employed for sam/bam format conversion and PCR duplicate read removal. RSeQC (version 2.6) was employed for read distribution analysis. The insert length was counted using Collect Insert Size Metrics tools from Picard software (version 2.8.2). DeepTools (version 2.4.1) was used to visualize the distribution of reads around TSS. MACS2 software (Version 2.2.7.1) was used for peak calling. Bedtools (version 2.30.0) was utilized for peak annotation and distribution analysis. Differential peaks were identified using csaw (version 1.24.3). The Homer (version 4.10) was utilized for motif analysis. Gene ontology (GO) analysis and Kyoto Encyclopedia of genes and genomes (KEGG) enrichment analyses for annotated genes were performed using KOBAS software (version 2.1.1), with a corrected P-value cutoff of 0.05 applied to determine statistically significant enrichment.

Statistical analysis and software

Differences between two sets of data were evaluated using a two-tailed Student's t-test, while comparisons among more than two groups were conducted using one-way ANOVA for human data analysis. Data were presented as mean and standard deviation (SEM). Statistical analyses were conducted using GraphPad Prism (GraphPad Software). A P-value less than 0.05 was considered statistically significant.

Supplementary Information

The online version contains supplementary material available at https://doi.org/10.1186/s13072-025-00586-6.

Supplementary Material 1.

Author contributions

L.Z., F.Z.,J.Z. and H.C. conceived and designed the experiments. L.Z., Y.X., J.H., Y.H., L.S., and N.S. performed the experiments, and H.C. provided new orbital tissue samples. L.Z. performed RNA-seq and CUT&Tag experiments. Y.X performed the bioinformatics analysis. L.Z., F.Z.,J.Z. and H.C. wrote the manuscript, with discussion and input from Q.J.

Funding

This work was supported by the National Natural Science Foundation projects of China (32000809 to L.Z.) and the National Science Foundation of Zhejiang Province (LY24 C120001 to L.Z.), Department of Science and Technology of Zhejiang Province (2024SSYS0021 to J.Z.), (2023C03036 to J.Z.), the National Natural Science Foundation projects of China (92357307 to F.Z.), (32171177 to F.Z.), the Open Project of the National Facility for Translational Medicine(Shanghai) (TMSK02021-103 to H.C.), the Fundamental Research Funds for the Central Universities (No.YG2023ZD17 to H.C.).

Data availability

Sequencing data have been deposited into the Gene Expression Omnibus (GEO) under the accession code GSE285862.

Declarations

Competing interests

The authors declare no competing interests.

Author details

[1]National Clinical Research Center for Eye Diseases, Shanghai General Hospital, Shanghai Jiao Tong University School of Medicine, Shanghai 200080, China. [2]Shanghai Key Laboratory of Fundus Diseases, Shanghai 200080, China. [3]Center for Stem Cell and Regenerative Medicine, Department of Basic Medical Sciences, and Bone Marrow Transplantation Center of the First Affiliated Hospital, Zhejiang University School of Medicine, Hangzhou 310000, China. [4]Center for Reproductive Medicine, The First Affiliated Hospital, Zhejiang University School of Medicine, Hangzhou 315300, Zhejiang, China.

Received: 3 October 2024 Accepted: 7 April 2025
Published online: 08 May 2025

References

1. Bahn RS. Current Insights into the Pathogenesis of Graves' ophthalmopathy. Horm Metab Res. 2015;47(10):773–8.
2. Longo CM, Higgins PJ. Molecular biomarkers of Graves' ophthalmopathy. Exp Mol Pathol. 2019;106:1–6.
3. Wang Y, Smith TJ. Current concepts in the molecular pathogenesis of thyroid-associated ophthalmopathy. Invest Ophthalmol Vis Sci. 2014;55(3):1735–48.
4. Smith TJ, Hegedüs L. Graves' disease. N Engl J Med. 2016;375(16):1552–65.
5. Bahn RS. Graves' ophthalmopathy. N Engl J Med. 2010;362(8):726–38.
6. Iyer S, Bahn R. Immunopathogenesis of Graves' ophthalmopathy: the role of the TSH receptor. Best Pract Res Clin Endocrinol Metab. 2012;26(3):281–9.
7. Dik WA, Virakul S, van Steensel L. Current perspectives on the role of orbital fibroblasts in the pathogenesis of Graves' ophthalmopathy. Exp Eye Res. 2016;142:83–91.
8. Tang QQ, Lane MD. Adipogenesis: from stem cell to adipocyte. Annu Rev Biochem. 2012;81:715–36.
9. Cristancho AG, Lazar MA. Forming functional fat: a growing understanding of adipocyte differentiation. Nat Rev Mol Cell Biol. 2011;12(11):722–34.
10. Obregon MJ. Adipose tissues and thyroid hormones. Front Physiol. 2014;5:479.
11. Cheng L, Hu J, Zhang L, Shen N, Chen H, Zhang F. Repurposing lenvatinib as a potential therapeutic agent against thyroid eye disease by suppressing adipogenesis in orbital adipose tissues. Pharmaceuticals. 2022;15(11):1305.
12. Berenson CS, Smith TJ. Human orbital fibroblasts in culture express ganglioside profiles distinct from those in dermal fibroblasts. J Clin Endocrinol Metab. 1995;80(9):2668–74.
13. Smith TJ, Bahn RS, Gorman CA. Hormonal regulation of hyaluronate synthesis in cultured human fibroblasts: evidence for differences between retroocular and dermal fibroblasts. J Clin Endocrinol Metab. 1989;69(5):1019–23.
14. Metzger E, Wissmann M, Yin N, Müller JM, Schneider R, Peters AH, Günther T, Buettner R, Schüle R. LSD1 demethylates repressive histone

marks to promote androgen-receptor-dependent transcription. Nature. 2005;437(7057):436–9.
15. Shi Y, Lan F, Matson C, Mulligan P, Whetstine JR, Cole PA, Casero RA, Shi Y. Histone demethylation mediated by the nuclear amine oxidase homolog LSD1. Cell. 2004;119(7):941–53.
16. Wang Y, Zhang H, Chen Y, Sun Y, Yang F, Yu W, Liang J, Sun L, Yang X, Shi L, Li R, Li Y, Zhang Y, Li Q, Yi X, Shang Y. LSD1 is a subunit of the NuRD complex and targets the metastasis programs in breast cancer. Cell. 2009;138(4):660–72.
17. Carnesecchi J, Forcet C, Zhang L, Tribollet V, Barenton B, Boudra R, Cerutti C, Billas IM, Serandour AA, Carroll JS, Beaudoin C, Vanacker JM. ERRalpha induces H3K9 demethylation by LSD1 to promote cell invasion. Proc Natl Acad Sci USA. 2017;114(15):3909–14.
18. Zhang L, Carnesecchi J, Cerutti C, Tribollet V, Perian S, Forcet C, Wong J, Vanacker JM. LSD1-ERRalpha complex requires NRF1 to positively regulate transcription and cell invasion. Sci Rep. 2018;8(1):10041.
19. Adamo A, Sesé B, Boue S, Castaño J, Paramonov I, Barrero MJ, Izpisua Belmonte JC. LSD1 regulates the balance between self-renewal and differentiation in human embryonic stem cells. Nat Cell Biol. 2011;13(6):652–9.
20. Duteil D, Metzger E, Willmann D, Karagianni P, Friedrichs N, Greschik H, Günther T, Buettner R, Talianidis I, Metzger D, Schüle R. LSD1 promotes oxidative metabolism of white adipose tissue. Nat Commun. 2014;5:4093.
21. Musri MM, Carmona MC, Hanzu FA, Kaliman P, Gomis R, Párrizas M. Histone demethylase LSD1 regulates adipogenesis. J Biol Chem. 2010;285(39):30034–41.
22. Hayami S, Kelly JD, Cho HS, Yoshimatsu M, Unoki M, Tsunoda T, Field HI, Neal DE, Yamaue H, Ponder BA, Nakamura Y, Hamamoto R. Overexpression of LSD1 contributes to human carcinogenesis through chromatin regulation in various cancers. Int J Cancer. 2011;128(3):574–86.
23. Schulte JH, Lim S, Schramm A, Friedrichs N, Koster J, Versteeg R, Ora I, Pajtler K, Klein-Hitpass L, Kuhfittig-Kulle S, Metzger E, Schüle R, Eggert A, Buettner R, Kirfel J. Lysine-specific demethylase 1 is strongly expressed in poorly differentiated neuroblastoma: implications for therapy. Cancer Res. 2009;69(5):2065–71.
24. Maniyadath B, Zhang Q, Gupta RK, Mandrup S. Adipose tissue at single-cell resolution. Cell Metab. 2023;35(3):386–413.
25. Mazitova AM, Marquez-Sanchez AC, Koltsova EK. Fat and inflammation: adipocyte-myeloid cell crosstalk in atherosclerosis. Front Immunol. 2023;14:1238664.
26. Ge K. Epigenetic regulation of adipogenesis by histone methylation. Biochim Biophys Acta. 2012;1819(7):727–32.
27. Chen L, Sun X, Chen D, Gui Q. LSD1 for the targeted regulation of adipose tissue. Curr Issues Mol Biol. 2022;45(1):151–63.
28. Douglas RS, Kahaly GJ, Patel A, Sile S, Thompson EHZ, Perdok R, Fleming JC, Fowler BT, Marcocci C, Marinò M, Antonelli A, Dailey R, Harris GJ, Eckstein A, Schiffman J, Tang R, Nelson C, Salvi M, Wester S, Sherman JW, Vescio T, Holt RJ, Smith TJ. Teprotumumab for the treatment of active thyroid eye disease. N Engl J Med. 2020;382(4):341–52.
29. Cao JM, Wang N, Hou SY, Qi X, Xiong W. Epigenetics effect on pathogenesis of thyroid-associated ophthalmopathy. Int J Ophthalmol. 2021;14(9):1441–8.
30. Duteil D, Tosic M, Lausecker F, Nenseth HZ, Müller JM, Urban S, Willmann D, Petroll K, Messaddeq N, Arrigoni L, Manke T, Kornfeld JW, Brüning JC, Zagoriy V, Meret M, Dengjel J, Kanouni T, Schüle R. Lsd1 ablation triggers metabolic reprogramming of brown adipose tissue. Cell Rep. 2016;17(4):1008–21.
31. Duteil D, Tosic M, Schüle R. Lsd1, a metabolic sensor of environment requirements that prevents adipose tissue from aging. Adipocyte. 2017;6(4):298–303.

Publisher's Note

Springer Nature remains neutral with regard to jurisdictional claims in published maps and institutional affiliations.